ELSEVIER

Earth and Planetary Science Letters 203 (2002) 165–180

EPSL

www.elsevier.com/locate/epsl

Massive barite deposits and carbonate mineralization in the Derugin Basin, Sea of Okhotsk: precipitation processes at cold seep sites

Jens Greinert [a,*], Sandra M. Bollwerk [b], Alexander Derkachev [c], Gerhard Bohrmann [a], Erwin Suess [a]

[a] *GEOMAR Research Center for Marine Geosciences, Wischhofstrasse 1–3, 24148 Kiel, Germany*
[b] *Graduate School 'Dynamics of Global Cycles within the System Earth', Wischhofstrasse 1–3, 24148 Kiel, Germany*
[c] *Pacific Oceanological Insitute, Far Eastern Branch of the Russian Academy of Sciences, POI, 43, Baltiyskaya Street, 690041 Vladivostok, Russia*

Received 27 December 2001; received in revised form 28 June 2002; accepted 9 July 2002

Abstract

An area of massive barite precipitations was studied at a tectonic horst in 1500 m water depth in the Derugin Basin, Sea of Okhotsk. Seafloor observations and dredge samples showed irregular, block- to column-shaped barite build-ups up to 10 m high which were scattered over the seafloor along an observation track 3.5 km long. High methane concentrations in the water column show that methane expulsion and probably carbonate precipitation is a recently active process. Small fields of chemoautotrophic clams (*Calyptogena* sp., *Acharax* sp.) at the seafloor provide additional evidence for active fluid venting. The white to yellow barites show a very porous and often layered internal fabric, and are typically covered by dark-brown Mn-rich sediment; electron microprobe spectroscopy measurements of barite sub-samples show a Ba substitution of up to 10.5 mol% of Sr. Rare idiomorphic pyrite crystals ($\sim$1%) in the barite fabric imply the presence of H_2S. This was confirmed by clusters of living chemoautotrophic tube worms (1 mm in diameter) found in pores and channels within the barite. Microscopic examination showed that micritic aragonite and Mg-calcite aggregates or crusts are common authigenic precipitations within the barite fabric. Equivalent micritic carbonates and barite carbonate cemented worm tubes were recovered from sediment cores taken in the vicinity of the barite build-up area. Negative $\delta^{13}C$ values of these carbonates (> -43.5‰ PDB) indicate methane as major carbon source; $\delta^{18}O$ values between 4.04 and 5.88‰ PDB correspond to formation temperatures, which are certainly below 5°C. One core also contained shells of *Calyptogena* sp. at different core depths with ^{14}C-ages ranging from 20 680 to $>$ 49 080 yr. Pore water analyses revealed that fluids also contain high amounts of Ba; they also show decreasing SO_4^{2-} concentrations and a parallel increase of H_2S with depth. Additionally, S and O isotope data of barite sulfate ($\delta^{34}S$: 21.0–38.6‰ CDT; $\delta^{18}O$: 9.0–17.6‰ SMOW) strongly point to biological sulfate reduction processes. The isotope ranges of both S and O can be exclusively explained as the result of a mixture of residual sulfate after a biological sulfate reduction and isotopic fractionation with 'normal' seawater sulfate. While massive barite deposits are commonly assumed to be of hydrothermal origin, the assemblage of cheomautotrophic clams, methane-derived

* Corresponding author. Tel.: +49-431-600-2122; Fax: +49-431-600-2911.
E-mail addresses: jgreinert@geomar.de (J. Greinert), sbollwerk@geomar.de (S.M. Bollwerk), pacific@online.marine.su (A. Derkachev), gbohrmann@geomar.de (G. Bohrmann), esuess@geomar.de (E. Suess).

PII: S0012-821X(02)00830-0

carbonates, and non-thermally equilibrated barite sulfate strongly implies that these barites have formed at ambient bottom water temperatures and form the features of a *Giant Cold Seep* setting that has been active for at least 49 000 yr.

Keywords: Okhotsk Sea; basins; barite; carbonates; hydrothermal vents; cold seeps; methane; sulfates; stable isotopes

1. Introduction

Cold seeps are sites of fluid expulsion, where authigenic minerals precipitate at the seafloor due to a variety of complex geochemical and biogeochemical reactions. Carbonates are probably the most common mineral precipitates at cold seeps and are well known from many locations at accretionary prisms and mud volcanoes around the world. Typically, carbonate formation is triggered by anaerobic oxidation of methane [1–4], which is transported from deeper sediment sequences via advecting fluids. Apart from carbonates, barite has also been observed at cold seeps [5–7]. Although less common than the formation of authigenic carbonate, it is understood now that barite forms by the interaction of Ba-rich and sulfate-free ascending fluids with dissolved sulfate of pore water in higher strata or the bottom water [8,9]. The dissolution of microcrystalline barite (e.g. bio-barite) in anoxic sediments – in which sulfate is exhausted by bacterial reduction – is assumed to be a major source for the Ba-enrichment observed in ascending fluids (e.g. [10]).

Both authigenic carbonate and massive barite deposits are known from the Derugin Basin in the Sea of Okhotsk (Fig. 1). Here, travertine-like barite was dredged in 1981 and 1986 from a ridge in 1460 m water depth. The results of these investigations were summarized by Astakhova et al. [11,12], who interpreted these barites to be of hydrothermal origin.

A sediment core taken in the same area in 1993 (Core 9310) also yielded small mixed barite-calcite precipitates [13]. Sedimentological, petrographic and isotopic analyses of these concretions, encrustations, and tube-like burrow-fillings of various shapes and sizes supported the assumption that methane-rich fluids played a role as carbon source in carbonate formation. Sulfur isotope analyses of barites clearly indicate the incorporation of microbially strongly fractionated sulfate, but oxygen isotopes of both carbonate and barite show no indications of temperate fluids or even hydrothermalism [13].

Based on this work, a more detailed investigation of the Derugin Basin area was carried out during the KOMEX project (Kurile–Okhotsk-Sea Marine Experiment) in 1998 (Cruise LV28) and 1999 (Cruise GE99) to ascertain the occurrence and activity of fluid venting and to elucidate the formation mechanism of the barite deposits in the Derugin Basin. In this paper we will present results from this project, which provide answers to the following questions: How do the barite deposits look in situ, and how large is the area of their deposition? What mechanism might be responsible for the barite formation? Is fluid venting still going on today and is there information available about the fluid venting history in the study area? Are there other mineral formations or gas emissions associated with the barite and carbonate precipitations which might help to determine whether these deposits were formed by hydrothermal activity or by the expulsion of cold fluids at a seep environment: *Cold Seep or Hydrothermal Vent*?

2. Study area and sampling strategy

The Derugin Basin is the major bathymetric feature in the central part of the Sea of Okhotsk, reaching a water depth of 1800 m. An asymmetric depression in the underlying basement causes the steep western flank of the basin to coincide with the eastern slope of Sakhalin Island (Fig. 1). In the north-western part the basin is filled with sediment up to 6 km thick, whereas the remaining area contains less than 3 km of sediment [14–

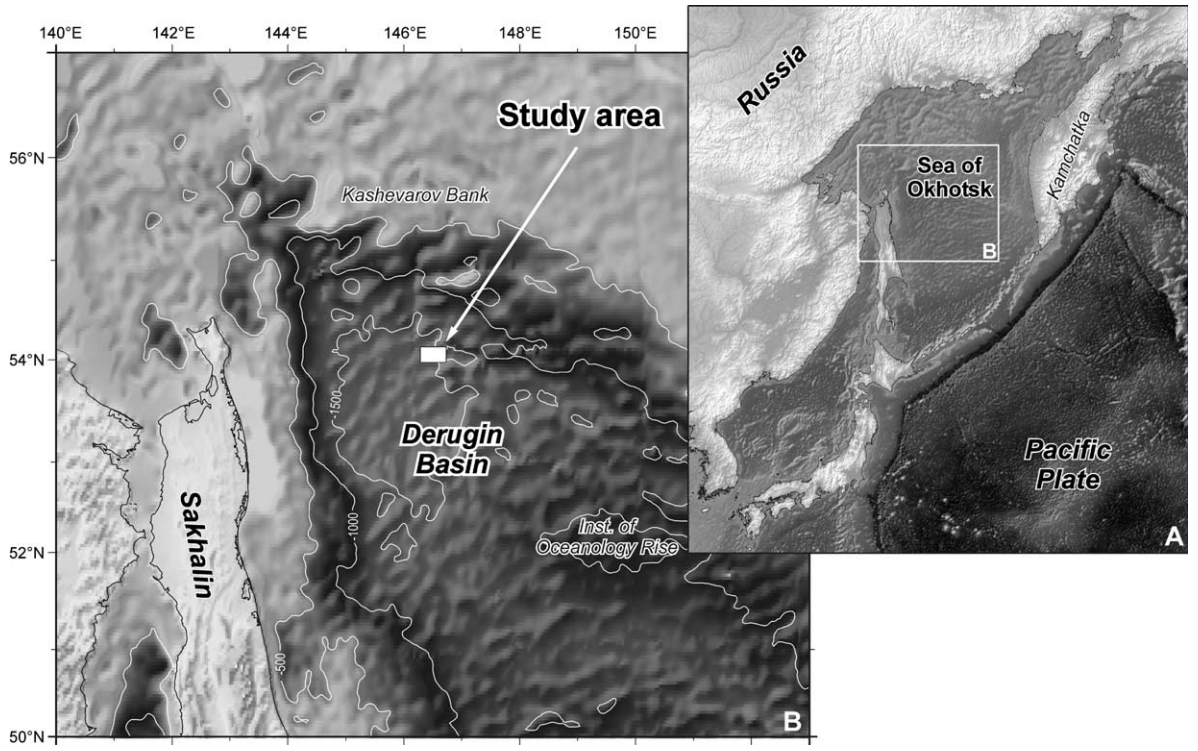

Fig. 1. Location of the Derugin Basin study area in the Sea of Okhotsk.

16]. Deeper strata are thought to be of Eocene–Oligocene age and are lying non-conformally above the basement. The uppermost Neogene–Quaternary sediments [14] contain considerable amounts of diatoms and radiolaria, reflecting the high primary productivity of the Sea of Okhotsk [17,18]. The tectonic origin of the Sea of Okhotsk and the nature of the basement are still uncertain [14–16]. The eastern flank is characterized by the presence of horst and graben structures, induced by NW–SE strike-slip faults and NE–SW thrusts and normal faults segmenting the basement (B. Baranov, personal communication).

At one of these horst structures [11–13], massive barite deposits were observed and sampled [19,20]. Bathymetric surveys [20] revealed a well-defined E–W trending ridge with a steep N-facing flank, which drops from 1420 m at the summit to 1650 m water depth at its base. The S-facing flank slopes more gently towards an area of uneven morphology with small ridges and depressions (Fig. 2). Here, sediments were retrieved by gravity coring (SLR 37-1; HYC 25-1) and direct video observations of the seafloor were carried out with a towed video and still camera-sled (OFOS; Ocean Floor Observation System). Based on these OFOS observations, dredge sampling was undertaken at the steep northward-dipping flank of the E–W striking ridge (DR 36-1) and at station DR 35-1. The two dredges recovered more than 100 kg of barite with several single blocks larger than 40 cm in diameter. Trawls for biological sampling as well as CTD/hydro-casts, particularly for methane analyses, completed our studies in the Derugin Basin.

3. Methods

The mineralogy and chemistry of barites were characterized by powder X-ray diffraction analyses (XRD; Philips PW 1820, monochromatic CoKα radiation), scanning electron microscopy (SEM; CamScan connected to an EDAX X-ray

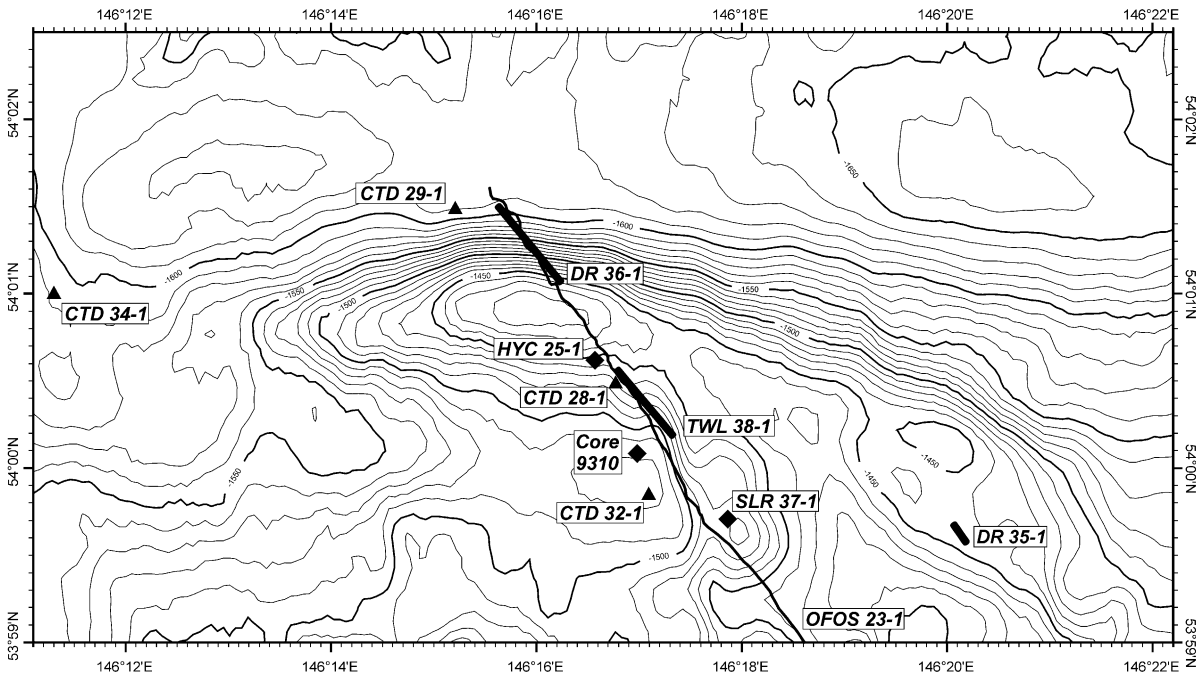

Fig. 2. Bathymetry of the studied area, Derugin Basin. NW–SE trending line marks the OFOS 23-1 observation track (53°59.170′N/146°18.457′E to 54°2.073′N/146°14.906′E). DR indicates dredge sampling (bold lines; DR 35-1 from 53°59.586′N/146°20.170′E to 53°59.666′N/146°20.079′E, DR 36-1 from 54°01.216′N/146°15.686′E to 54°00.780′N/146°17.395′E) and trawl sampling (TWL 38-1 from 54°00.052′N/146°17.514′E to 54°01.288′N/146°16.267′E); diamonds are sediment coring sites (SLR 37-1 at 53°59.796′N/146°17.830′E; HYC 25-1 at 54°00.844′N/146°16.649′E; Core 9310 from previous work [13]); CTD/hydrocasts are depicted as triangles.

microanalyzer), and electron microprobe spectroscopy (EMS; Cameca SX 50). Acceleration voltage for EMS was 15 kV at a 10 nA beam current; the counting intervals varied from 20 to 40 s depending on the element analyzed. Measurement deviations were less than 1% for sulfate, sulfide and carbonate standards. The texture and morphology of the barites were studied macroscopically, using light microscopy, and by SEM.

$\delta^{34}S$ investigations of barite samples were carried out at the University of Bochum (Delta S Finnigan) following the method of Yanagisawa and Sakai [21]. The oxygen isotopes of the barite sulfate were analyzed at the University of Calgary. Samples were ground with graphite and heated to 1100°C; the escaping CO_2 was trapped and measured with a Finnigan 251. Values for $\delta^{34}S$ are given relative to the CDT standard; $\delta^{18}O$ values are reported relative to SMOW. Strontium isotope ratios were measured on acid leachates at the University of Bochum (Finnigan MAT 262); strontium was separated on cation exchange columns with 2.5 N HCl and dried at 120–150°C before analyzing.

→

Fig. 3. (A–C) The seafloor in the Derugin Basin study area observed during OFOS 23-1 (white bars = 40 cm). White irregular and porous barite occurs as debris (A,C) and as build-ups of up to 10 m in height and similar in diameter. Between these build-ups typical patches of *Calyptogena* sp. indicate active venting of H_2S-rich fluids (B). The dredged barite samples (D–F) show a very porous fabric. Larger fluid channels are marked by an arrow; in (D), one of these channels is visible as a brown-coated larger pore in the center of the image continuing into the upper left corner. (F) Layered structures which point to a periodic barite precipitation and growth of the build-ups. The seafloor observation and the nearly sediment-free barite fabric strongly suggest a formation above the sediment surface and a growth of the barite build-ups into the water column.

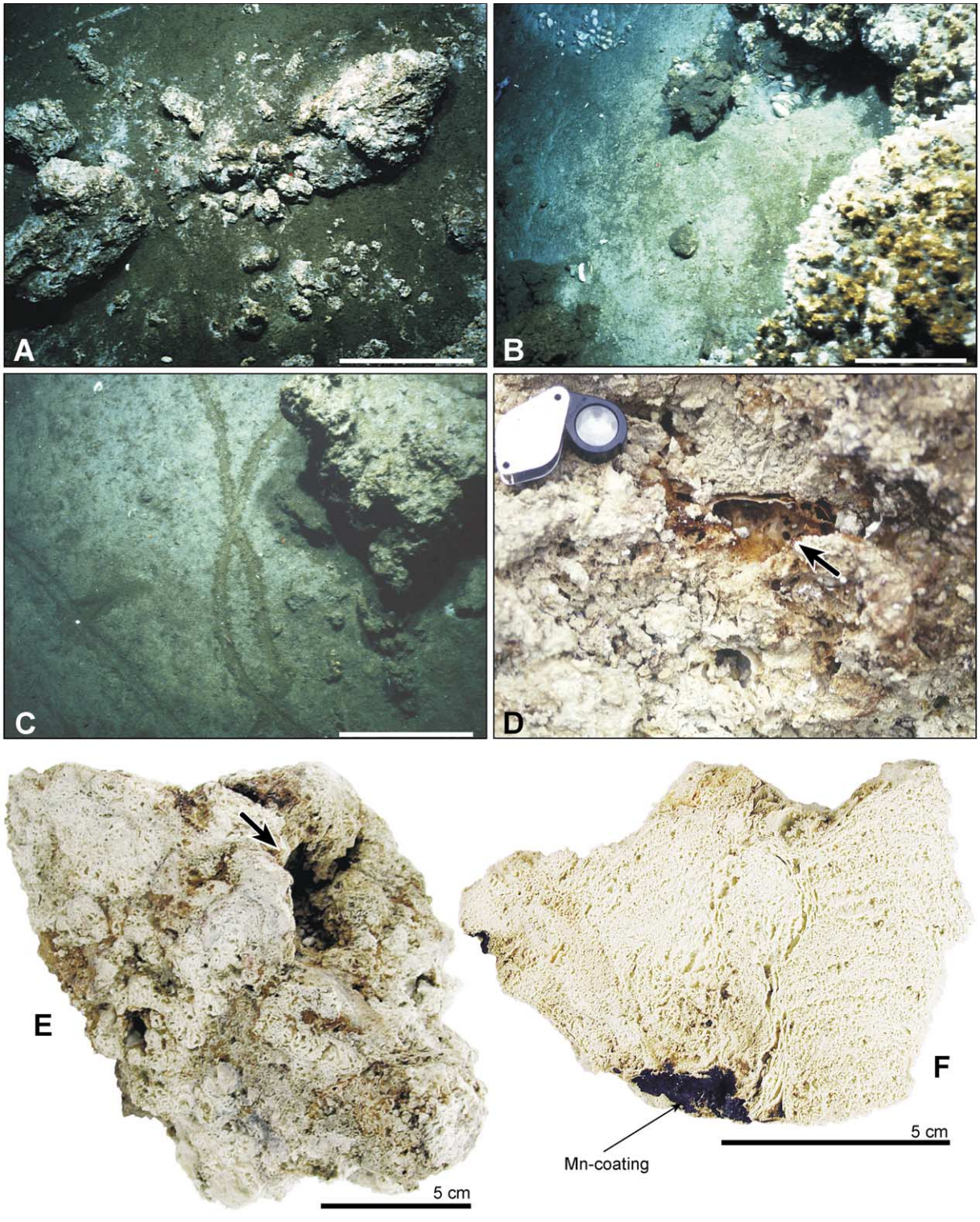
A
B
C
D
E
5 cm
F
5 cm
Mn-coating

The CO_2 extraction for $\delta^{13}C$ and $\delta^{18}O$ measurements of carbonates was carried out with pure H_3PO_4 at 75°C with a Carbo-Kiel on-line device connected to a Finnigan MAT 252. All carbonate isotope values are given relative to PDB. Age determinations by ^{14}C analyses of clam shells were carried out by the AMS facility at the Leibniz Laboratory in Kiel. Methane analyses of water samples were carried out on board by gas chromatography, using a specific vacuum system for the gas extraction [22]. Pore water was squeezed on board and the amount of NH_4 was determined using a photometric auto-analyzer. Sulfate and barium were measured in the shore-based laboratory by ion-chromatography and ICP-OES, respectively, following established procedures (for detailed method description see: http://www.geomar.de/zd/labs/labore_umwelt/Meth_englisch.html).

4. Results and discussion

4.1. Direct signs of active fluid venting

The deployment of OFOS 23-1 in the Derugin Basin yielded the first direct seafloor observations for this area. Along the track of about 3.5 km length, whitish, irregular blocks of up to 1 m in size were randomly observed on the sediment surface or half buried in the sediment (Fig. 3A). In places, they appeared more spectacularly as reef-like blocks or build-ups of up to 10 m in height with rather irregular surfaces (Fig. 3B). Both the randomly distributed blocks and the larger build-ups consisted of extremely porous material typically covered by a thin gray to dark brown layer. The dredged samples (DR 36-1 and 35-1) showed that this irregular mass is almost pure barite. Larger barite build-ups were found along the entire OFOS track with 10–100 m wide areas of soft and strongly bioturbated sediment in between (Fig. 3C). In these sedimented areas signs of active fluid venting were found in small fields of living individuals of *Calyptogena* sp. (Vesicomyidae), which were often observed close to larger barite build-ups (Fig. 3B). In addition to *Calyptogena* specimens, shells of *Acharax* sp. (Solemyidae) were recovered by trawling. All vesicomyid and solemyid bivalves investigated so far depend on the symbiosis with chemoautotrophic endosymbiotic bacteria [23]. The occurrence of both species is restricted to areas of reduced geochemical conditions directly below the sediment surface. Their occurrence in this area strongly supports a recent hydrogen sulfide-rich fluid flux at least at small-scale focused sites (~1 m size) observed along the entire track.

4.2. Porous barites with travertine-like fabric

The irregular surfaces of the barites resemble a travertine-like fabric with meso- and mega-pores occupying approximately 40 vol% (Fig. 3D). In some of the larger pores, up to several centimeters in size, similar thin barite layers occur as rim cements of the pores or as fragile 'barite-leaves' in the center of the pore. Both fabrics represent secondary fillings, suggesting that larger pores were pathways for fluids which migrated through the whole barite fabric. In cross cut, the general fabric exhibits layers of less than 1 mm in thickness, often arranged sub-parallel and spaced less than 2 mm from each other. These fabric areas indicate a step-like growth of the whole barite fabric. Other areas show a more isotropic, still very porous barite crystallization (Fig. 3F).

As recognized by seafloor observations, the sur-

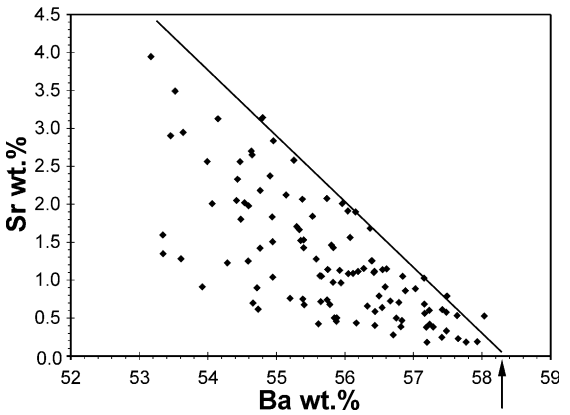

Fig. 4. EMS analyses show variable Ba substitution by Sr of up to 4 wt%. The stoichiometric Ba amount for pure Ba sulfate is shown by an arrow. The line describes the weight ratio for a stoichiometric Ba–Sr sulfate.

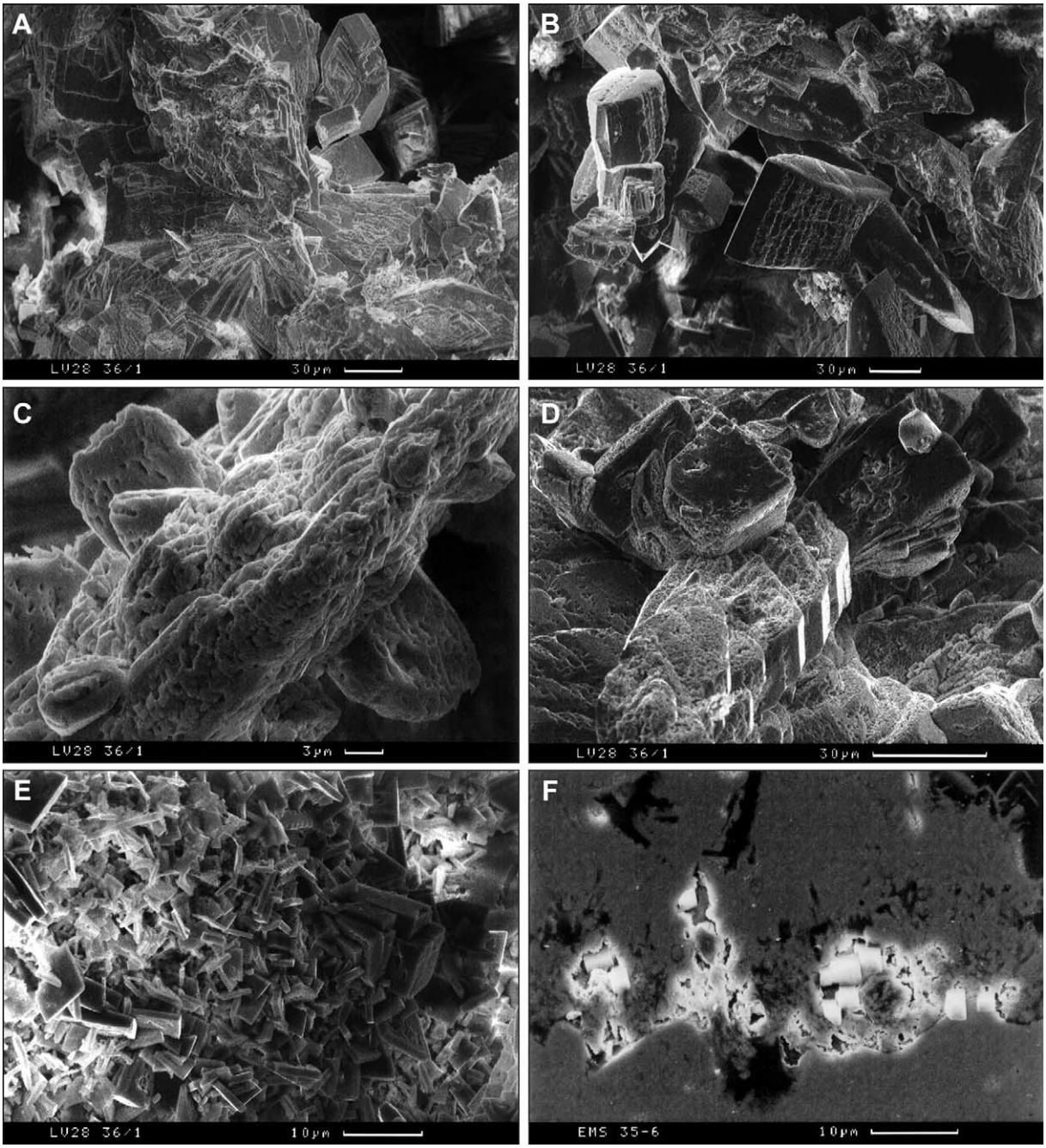

Fig. 5. SEM images of barite samples; (A,B) represent typical barite crystal shapes; (C) shows usual twinning and possible solution features, whereas the 'amorphous mass' in (D) is possibly a result of fast precipitating barite. (E) Unusual plate- and needle-shaped barite crystals with diatom shell fragments (arrow). (F) Idiomorphic pyrite crystals in a thin section which was used for EMS analyses.

faces of the outcropping blocks are often coated by dark brown or gray sediment, whereas the barite itself varies in color from pale white to yellow. The sediment coating consists of silt and clay-sized terrigenous material with high amounts of siliceous plankton (diatoms and radiolaria). EDS investigations show Mn-enrichment, which probably causes the dark brown color, but XRD analyses did not provide any evidence of a crystalline, Mn-containing mineral phase.

XRD analyses of bulk samples from different blocks show barite as monomineralic phase. A shift of 0.01 and 0.004 Å of all reflections to smaller *d*-spacing indicates Sr substitution for Ba in the barite lattice. This was confirmed by EMS and EDS investigations, which yielded a Ba replacement of up to 10.5 mol% Sr (equivalent to 4 wt% Sr; Fig. 4). Additional thin sections and SEM investigations show opaque, cubic pyrite crystals (2 and 6 μm) or clusters of pyrite crystals, which are distributed in the barite fabric at random (Fig. 5F).

The SEM investigations also yielded images of a very porous micritic barite fabric (Fig. 5A,B). Many crystals consist of plates forming a spire- and rhomb-like habitus (Fig. 5A,D) and show twinning (Fig. 5B,C). Others show rings of pseudo-hexagonally arranged prism faces filled by a xenomorphic barite mass (Fig. 5D). Many crystal faces exhibit uneven surfaces with pits and a wavy structure which resemble dissolution features (Fig. 5C). However, the generally idiomorphic crystals clearly indicate growth without space limitation. This and the porous, nearly sediment-free barite fabric itself strongly support a barite formation in the bottom water. Fluid migration through the barite makes the barite formation at the edge of the build-ups possible.

In addition to the barite, one small light yellow crust was recovered which was tightly cemented into the barite fabric of one edifice from station DR 35-1. XRD analyses showed aragonite to be the only crust-forming mineral there. Furthermore, we found shells of *Calyptogena* sp. and *Provanna* sp. (Gastropoda), which were also incorporated in the barite fabric of dredged and cored barite samples. The shells are coated with different cement generations of barite. Living evidence for the migration of H_2S-rich fluids through the barite fabric is given by frequently observed clusters of thin red pogonophora tube worms settling in larger pore spaces. These tube worms are less than 2 mm in diameter and up to 10 cm long and belong to the family *Sclerolinidae* (Monilifera, Pogonophora; H. Sahling personal communication). Their C and N isotope composition indicates chemoautotrophic nutrition and confirms our inference of recent active venting of H_2S-rich fluids.

Macroscopically, the barites recovered from the Derugin Basin are very similar to other cold seep-associated barites, e.g. in Monterey Bay [7], the

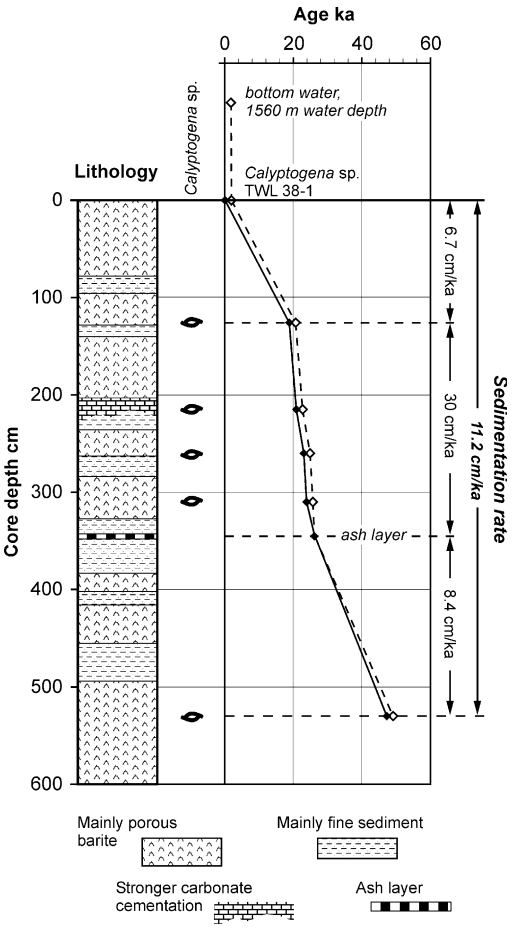

Fig. 6. Lithology of Core SLR 37-1 with ^{14}C ages of shells from *Calyptogena* sp. (open diamonds are original ^{14}C ages, whereas the solid diamonds are corrected for a bottom-water value of 1850 yr), and calculated sedimentation rates.

Gulf of Mexico [8], the Peruvian Margin [10] or the San Clemente Basin [24]. They also show some resemblance to hydrothermal barites from the Mariana Trough [25]. Microscopically, the spire- and rhomb-like crystal habitus of our Derugin Basin samples is equivalent to those described by Nähr et al. [7] and Lonsdale [24], but the crystals differ from the concentric layers and dendritic/rosette-shaped barites described by Torres et al. [10] or Fu et al. [8].

4.3. Carbonate precipitates and venting history

The first answers to questions on the fluid venting environment and its history in the Derugin Basin came from a sediment core recovered close to OFOS track 23-1 (Fig. 2). The 6 m long core SLR 37-1 consisted of hemipelagic sediment interbedded with nearly pure barite horizons (Fig. 6). The barite found here was the same in texture and mineralogy as the dredged barite samples but with more sediment filling the porous fabric. The composition of this pore-filling sediment is the same as that of sediment horizons in Core SLR 37-1 and Core HYC 25-1 sampled 2 km northward (Fig. 2). The sediment of both cores represents a diatomaceous mud containing small fragments of barite debris of mm to cm size, micritic barite crystals and small dark grayish tubes of less than 3 cm in length and less than 2 mm in diameter. These tubes consist of barite and/or carbonate cemented sediment. Their appearance is iden-

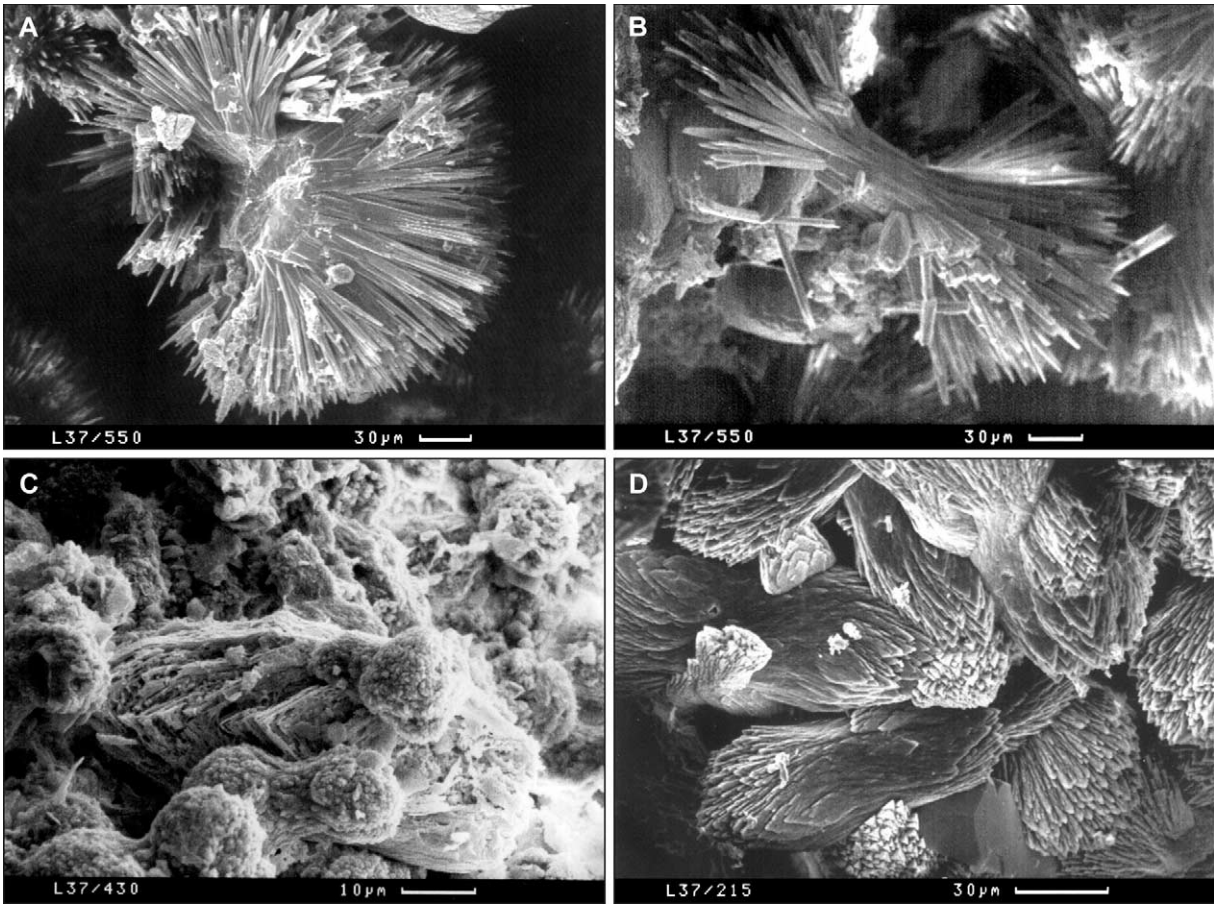

Fig. 7. SEM images of aragonite (A,B) and Mg-calcite (C,D) precipitates found in Core SLR 37-1. Their shapes point to biogenic formation. Samples in (A,B) are from 550 cm, (C) from 430 cm and (D) from 215 cm core depth.

Table 1
AMS ^{14}C ages of clam shells found in Core SLR 37-1

Core depth	Age BP (yr)
Sediment surface (clam, TWL 38-1)	1 935 ± 30
126 cm (clam)	20 680 ± 110
215 cm (clam)	22 750 ± 130
260 cm (clam)	24 890 ± 200
310 cm (clam)	25 710 ± 180
342 cm (ash layer)	26 800
530 cm (clam)	> 49 080

One shell from trawl TWL 38-1 was taken for the carbonate age of a 'recently' living clam.

tical to those manifestations recently interpreted by Derkachev et al. [13] as cementations of worm tubes (Core 9310). The carbonate in both cores also occurs as aggregates of micritic aragonite and Mg-calcite. It frequently forms dumbbells and spheres (Fig. 7) with a great similarity to biologically induced precipitations [26,27]. Carbonate is also present in the barite fabric from different depth intervals of Core SLR 37-1. Here, Mg-calcite crystallizes as a secondary pore cement of dumbbell shape, indicating a biogenically induced precipitation as well (Fig. 7).

The generally higher carbonate content in Core SLR 37-1 increased below 200 cm core depth and culminated in a solid carbonate crust within a strongly bioturbated horizon between 200 and 220 cm (Fig. 6). Within this horizon, shells and shell fragments of *Calyptogena* sp. were found. Microscopically, the carbonate content also increased at 126, 260, 310 and 530 cm, where clam shells were found as well. The occurrence of clam shells down to 530 cm in Core SLR 37-1 suggests that active fluid venting had occurred, permanently or episodically, for a long time at or very close to the coring location, which allowed the clams to live. To estimate the age of the fluid venting at the coring site SLR 37-1, we measured ^{14}C on clam shells from all five horizons (Table 1). In addition, we analyzed a well-preserved clam shell from the sediment surface recovered by trawling TWL 38-1 (Fig. 2) as well as bottom water from 1561 m water depth sampled slightly north of the studied area. Both the clam shell from TWL 38-1 (1935 ± 30 yr) and the bottom water (1850 ± 30 yr) show nearly the same age (Table 1), indicating that 'recently' living clams indeed reflect the ^{14}C age of the bottom water. We corrected the ^{14}C ages of the clams from Core SLR 37-1 by subtracting the recent bottom water age of 1850 yr and calculated the 'real' age

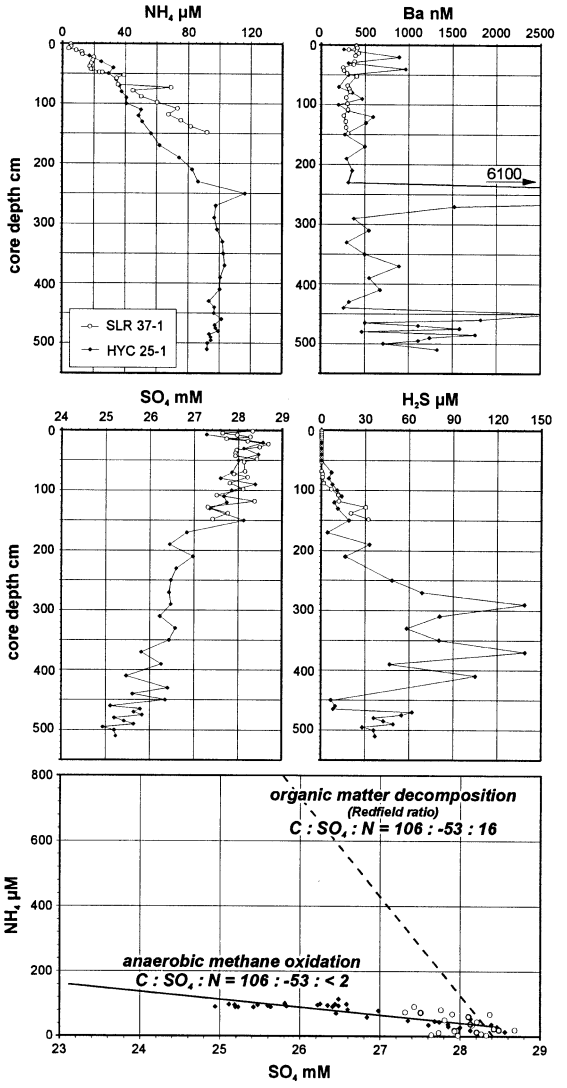

Fig. 8. Pore water analyses from Core SLR 37-1 (black diamonds) and HYC 25-1 (open circles). Extreme Ba concentrations indicate Ba-rich fluids, which are transported in definite pathways through the porous barite fabric. Decreasing SO_4^{2+} and increasing H_2S concentrations point to in situ sulfate reduction processes and a transport of both components from deeper sediment horizons up to the sediment surface. The low NH_4 concentrations and their relation to the decreasing sulfate indicate methane is oxidized via sulfate reduction.

of the clams at the deepest horizon to be approximately 47 230 yr (Fig. 6). The clam age data agree with the age of an ash layer at 342 cm core depth. This layer was identified by mineral analyses as the rhyolithic ash layer K_2, which occurs throughout the Sea of Okhotsk and is known to be 26 800 years old [20,28].

4.4. Barite formed from biogenically reduced sulfate

Seafloor observations and the porous, mostly sediment-free barite fabric suggest that the barite growth takes place within the bottom water. Barite formation is induced by the reaction of Ba-rich, sulfate-depleted, discharging fluids with sulfate-rich bottom water. Pore water analyses of barium from Core SLR 37-1 show concentrations of up to 6100 nM, which is more than 10 times the normal background value measured in Core HYC 25-1 (Fig. 8). The erratic occurrence of high Ba concentrations in Core SLR 37-1 points to fluids which flow through definite pathways of the porous barite fabric. Decreasing sulfate concentrations with depth and the parallel increase of hydrogen sulfide strongly suggest that sulfate reduction triggers the barium release at deeper sediment horizons. To confirm this assumption and investigate possible hydrothermal influences, we analyzed the S and O isotope signature of barite sub-samples. Isotope values range between 8.4 and 15.9‰ in $\delta^{18}O$ SMOW and between 21.0 and 38.6‰ in $\delta^{34}S$ CDT for pure barite samples (Table 2). The barite cemented worm tubes of Core SLR 37-1 are similar in range except for one sample which shows a significantly higher $\delta^{34}S$ value. Samples from Core HYC 25-1 are higher in both $\delta^{34}S$ and $\delta^{18}O$, with values similar to those typically found in Core 9310 [13] (Fig. 9).

The isotopic composition of sulfate in the marine environment is controlled by the temperature-induced equilibration between sulfate and the surrounding water as well as by biogenic fractionation during sulfate reduction. Sulfate reduction influences both the O and S isotopic compositions (e.g. [3,29–33]), whereas temperature influences only oxygen [34]. According to Claypool et al. [35], microbial reduction of seawater sulfate follows a $\delta^{34}S/\delta^{18}O$ ratio of 4 (Fig. 9). S and O isotope values that deviate from this ratio are interpreted either as re-equilibrated with H_2O at higher temperatures [34,36] or influenced by re-oxidized H_2S [37]. More recent studies [3,29,33] show that the fractionation factor of O and S is influenced by the microbial sulfate reduction rate and the initial sulfate concentration in the pore water, which changes the isotopic composition of the residual sulfate and the released H_2S. Aharon and Fu [3] showed that even at equivalent *P–T*

Table 2
S, O and Sr isotopic data from barite build-ups (DR samples) and small barite cemented worm burrows found in the sediment of Core SLR 37-1 and HYC 25-1

	$\delta^{18}O$ (‰ SMOW)	$\delta^{34}S$ (‰ CDT)	$^{87}Sr/^{86}Sr$	Core depth (cm)
DR 36-1	9.0	24.7	0.708832	
	9.6	21.0	0.708735	
	10.8	27.3	0.708656	
	12.4	26.8		
	12.8	24.6		
	13.6	33.0	0.708684	
	14.2	29.6		
	15.0	29.2		
	15.2	30.9		
	15.4	33.6	0.708643	
	15.8	34.9		
	15.9	33.7	0.708654	
	16.1	33.2		
	16.5	34.6		
	17.2	38.6		
	17.6	32.4		
DR 35-1	12.9	23.5		
	13.7	26.5		
	14.1	31.9		
	14.2	29.2		
	14.3	29.1		
	14.3	28.4		
	14.6	31.5		
	14.8	30.3		
	15.3	30.6		
	15.8	35.2		
SLR 37-1	9.7	22.6		5
	11.2	21.9		135
	17.3	55.0		215
	10.1	21.2		320
	11.7	23.3		440
	12.3	24.1		535
HYC 25-1	20.1	62.2		50
	19.7	75.4		75
	20.0	77.1		85
	20.5	73.9		155

conditions, the $\delta^{34}S/\delta^{18}O$ ratios from different sites vary between 3.5 and 1.4, the latter measured at a non-venting reference site. They argue that these ratios indicate that kinetic isotope effects *exclusively* control both the sulfur and oxygen isotope fractionations during microbial sulfate reduction. Our dredged barite samples (black symbols in Fig. 9) plot along a line with a $\delta^{18}O/\delta^{34}S$ ratio of 2.1, the same ratio found at cold seeps in the Gulf of Mexico [3]. A thermal equilibration at 100–200°C [34] could explain the oxygen isotopic signal of our dredged barite. However, this temperature influence cannot explain the parallel change in the sulfur isotope data.

Barite of cemented worm tubes from both sediment cores discussed here and the analyses of Core 9310 presented by Derkachev et al. [13] undoubtedly show that microbially fractionated residual sulfate has been incorporated into the barite. Hence, these data support our postulate that microbial sulfate reduction in the Derugin Basin sediment occurs in a closed or semi-closed system, generating sulfate that is strongly enriched in ^{34}S and ^{18}O. The minor enrichment of ^{34}S and ^{18}O within the dredged barites can be explained by higher amounts of incorporated bottom water sulfate, due to the formation at the edges of the barite build-ups, that is not enriched in ^{34}S and ^{18}O. Furthermore, we believe that the observed deviation from the $\delta^{34}S/\delta^{18}O$ ratio of 4 reflects kinetic fractionation [3] and does *not* indicate a significant temperature increase.

4.5. Methane venting and carbonate formation

Methane analyses of sediment and water samples carried out on board already indicated the origin of carbonate in the Derugin Basin. Higher amounts of methane were detected in the sediment of Core SLR 37-1, but significant methane concentrations of up to 5700 nl/l measured at three CTD stations (CTD 28-1, 29-1, 32-1; Fig. 2) in more than 1300 m water depth support the hypothesis of active venting of methane-enriched

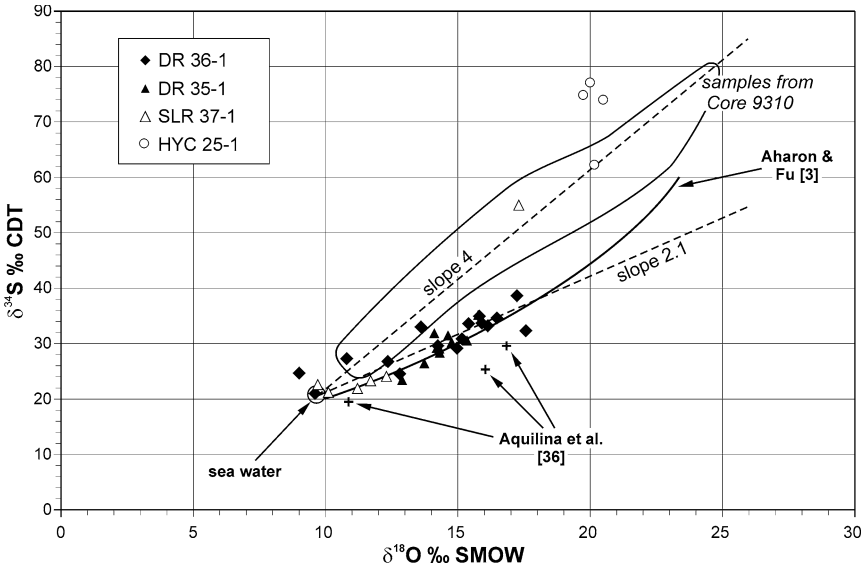

Fig. 9. S and O isotope analyses of barite samples from dredge (black symbols) and core samples (white symbols). Theoretically, the O-isotope data represent a sulfate equilibration with the surrounding water (0‰ SMOW) at 100–200°C. A sulfate equilibration at the measured bottom-water temperature of 2°C in the Derugin Basin results in $\delta^{18}O$ values of 38‰ SMOW [34]. Assuming a temperature-driven equilibration, Aquilina et al. [36] interpreted their data (black cross) from the Peruvian Margin as equilibrated at temperatures higher than 100°C. Suggested from more recent investigations at cold gas and oil seeps in the Gulf of Mexico (solid line, [3]), our barite data (trending along a line with a slope of 2.1) can be assumed to be residual sulfate which was isotopically changed during microbial sulfate reduction *only*. Such microbial changes were primarily thought to result in a 'constant' fractionation which is 4 times higher in S than in O (dashed line with slope 4).

fluids [19,20]. The methane-free bottom water at station CTD 34-1 west of OFOS track 23-1 probably marks the boundary of the active venting region (Fig. 2). Carbon isotope values of the aragonite crust from station DR 35-1 and tube-like carbonate samples recovered from core sampling indicate a precipitation formed from bacterial oxidation of methane-rich fluids [1,4]. The crust shows $\delta^{13}C$ values ranging from −40.7 to −42.9‰; analyses of the small tube-like carbonate aggregates from Core SLR 37-1 and HYC 25-1 yield $\delta^{13}C$ values between −16.4 and −43.5‰ (Table 3). Nevertheless, they are clearly methane-related as well and similar in range to those reported for similar carbonates from Core 9310 ($\delta^{13}C$ from −37.6 to −42.9‰) [13].

Geochemical pore water analyses of both cores confirmed the expulsion and reoxidation of methane as indicated by the SO_4/NH_4 ratio. If oxidation of organic matter via sulfate reduction were exclusively responsible for the observed SO_4 depletion of 3.5 mM, more than 800 μM of ammonia should be present in the pore water. If we compare this SO_4/NH_4 ratio to a reaction of 53 mol SO_4 with organic matter of a Redfield composition, less than 2 mol NH_4 would have been released (Fig. 8). This is much less than the expected 16 mol of NH_4 that should be released by this reaction. Thus, an additional substrate devoid of nitrogen must be involved in the sulfate-decreasing mechanisms.

Table 3
Carbon and oxygen isotopic data of carbonates from Core SLR 37-1, HYC 25-1 and an aragonite crust from station DR 35-1

	$\delta^{18}O$ (‰ PDB)	$\delta^{13}C$ (‰ PDB)	Core depth (cm)
SLR 37-1	5.47	−43.3	165
	5.61	−44.6	195
	5.49	−42.2	202
	5.88	−43.5	215
	5.85	−42.2	215
	4.82	−19.0	420
	4.81	−17.4	440
	4.04	−16.4	440
	4.50	−29.5	510
HYC 25-1	4.77	−40.57	75
DR 35-1	4.53	−38.3	
	4.56	−40.1	

Methane oxidation via sulfate reduction explains this sulfate decrease and is well known from other cold seep locations (e.g. [38]). The predominant methane generation mechanism – biogenic or thermogenic – cannot be ascertained solely on our C isotope data. Because of the high primary production in the Sea of Okhotsk it is likely that biogenic methane is produced at shallow depths in the sediment in any case. A thermogenic origin of at least some of the methane is also likely, as gas and oil deposits are well known from the Sakhalin Shelf. Values higher than −25‰ $\delta^{13}C$ in carbonates from Core SLR 37-1 probably represent a mixture of ascended, methane-derived carbon, CO_2 generated from organic matter degradation and the bottom water-dissolved inorganic carbon. However, the incorporation of HCO_3^- released from the anaerobic methane oxidation via sulfate reduction [1,4] can be assumed safely as the dominant carbon source for the aragonite and Mg-calcite precipitation within the sediment and the barite pore spaces. As for the barite, the oxygen isotope data of the carbonates contribute significantly to answering the question '*Cold Seep or Hot Vent*?'. With values between 4.04 and 5.88‰ (Table 3) the corresponding formation temperature is certainly below 5°C, regardless of whether aragonite, calcite or Mg-calcite was precipitated [6].

4.6. Sr isotopes and depth estimate of the fluid source

The Sr isotope ratio $^{87}Sr/^{86}Sr$ of different samples from DR 36-1 provides more information about the mixing ratio between ascending fluids and bottom water and the possible age of the ascending fluids. With $^{87}Sr/^{86}Sr$ ratios of 0.708643–0.708832 (Table 2) the barites are significantly lighter than the recent seawater in the Sea of Okhotsk, with values between 0.70917 and 0.70910 (the latter from [39]) and the global seawater value of 0.709175 [40]. Carbonates from Core 9310 with $^{87}Sr/^{86}Sr$ ratios between 0.708260 and 0.708722 are even more depleted in ^{87}Sr. They ascertain that Sr in both authigenic barite and carbonate is predominantly provided by the upward migrating fluids which interacted with ma-

terial of low Sr ratios. Dacitic or rhyolithic tuffs (0.7033–0.7036 $^{87}Sr/^{86}Sr$), which are known from the Sea of Okhotsk [39], are one possible material. At least one well visible ash layer of rhyolithic composition (K_2) in core SLR 37-1 [20,25] supports the hypothesis of solution processes of ash particles with low Sr ratios that could change the Sr isotopic composition of ascending fluids [41] at cold seeps in the study area.

Considering the global 'age curve' for Sr in the oceans [40], the barite Sr ratios correspond to an age of 8–16 Ma. This age is definitely too old to be the age of the barite precipitation, but it may represent the age of deep-derived fluids that were involved in the barite formation. If this was the case, the source depth of such deep-derived fluids can be estimated using sedimentation rates in Core SLR 37-1 derived from clam and ash ages. The sedimentation rate thus obtained varies from 6.7 to 30 cm/ka, with a mean rate of 11.2 cm/ka (Fig. 6). This value is in agreement with estimates based on oxygen isotope and ^{14}C analyses of foraminifera from other core locations in the Derugin Basin (R. Tiedemann, unpublished data) that yield sedimentation rates of 7–15 cm/ka. The high rate of 30 cm/ka might be caused by a higher amount of barite debris deposited near a large barite build-up. It may also reflect a period of increased fluid flow 20 700–26 800 yr ago, which forced a more rapid in situ formation of barite. If we assume that the Sr isotope data of the barites indicate deep-seated fluids and that sediments are deposited at a rate of 11.2 cm/ka (Fig. 6), then we can infer a fluid source depth of 900–1800 m below the seafloor. Unfortunately, our data cannot be used to unambiguously discern whether deep-derived fluids, dissolution processes of ash layers, or a combination of both processes have caused the Sr isotope ratios of the barite and carbonate precipitates from the Derugin Basin, but they provide first ideas from which depth deep-derived fluids may come from.

5. Conclusion

Venting of Ba- and methane-rich fluids induced the barite precipitation of pillar- to block-like barite build-ups several meters high and small carbonate deposits in the sediment and the barite pore space. Barite build-ups grew at their edges when Ba came in contact with higher amounts of sulfate. A fraction of this sulfate is enriched in ^{34}S due to isotopic fractionation during biological sulfate reduction. One possible source of this residual sulfate might be the porous barite fabric itself. The paragenesis of carbonates generated by microbially mediated methane oxidation points to in situ sulfate reduction within the barite fabric. The occurrence of authigenic pyrite crystals and chemoautotrophic tube worms further indicates the presence of H_2S. Hydrogen sulfide is also a component of the Ba-transporting fluids that ascend from deeper sediment horizons. Small fields of living clams (*Calyptogena* sp.) at the seafloor and the chemoautotrophic tube worms in the porous barite fabric provide clear signs of recently active fluid venting in the Derugin Basin.

Sulfur and oxygen isotope analyses of the barite, the co-occurrence of methane-derived carbonates and their oxygen isotope signature indicate that barite and carbonate formation is related to cold fluid venting. This suggestion is strongly supported by the absence of clay minerals such as nontronite, other Fe-smectites or the Mn-oxide todorokite. Although these minerals are usually found in marine hydrothermal environments [42], they are completely absent from the Derugin Basin sites. Because of the widespread occurrence of barite deposits on the seafloor (steadily observed along a 3.5 km long track and sampled within an area of 32 km^2), the amount of deposited barite in up to 10 m high build-ups and the detection of methane anomalies in the water column corroborate our assumption that the studied area represents a *Giant Cold Seep* setting that has been active – constantly or periodically – for at least 47 230 yr.

Acknowledgements

We kindly thank all the people on board RV *Lavrentyev* and RV *Gelovany* for their great help in handling the scientific equipment and for the fast and professional chemical analyses on board

and afterwards on shore. Furthermore, we would like to thank all our Russian colleagues for their enthusiasm during these cruises and our stay in Vladivostok. We also thank H. Strauß and P. Grootes for isotope analyses, E. Hütten, A. Obzhirov, H. Sahling, R. Tiedemann for essential input as well as M. Torres and W. Moore for their thorough and careful reviewing. Our thanks go to the Federal Ministry of Education and Research, Bonn, for supporting this work (Grant 03G0535A).*[BOYLE]*

References

[1] S. Ritger, B. Carson, E. Suess, Methane-derived authigenic carbonates formed by subduction-induced pore-water expulsion along the Oregon/Washington margin, Geol. Soc. Am. Bull. 98 (1987) 147–156.

[2] H. Sakai, T. Gamo, Y. Ogawa, J. Boulégue, Stable isotopic ratios and origins of the carbonates associated with cold seepage at the eastern Nankai Trough, Earth Planet. Sci. Lett. 109 (1992) 391–404.

[3] P. Aharon, B. Fu, Microbial sulfate reduction and sulfur and oxygen isotope fractionations at oil and gas seeps in deep water Gulf of Mexico, Geochim. Cosmochim. Acta 64 (2000) 233–246.

[4] J. Greinert, G. Bohrmann, E. Suess, Gas hydrate-associated carbonates and methane-venting at Hydrate Ridge: Classification, distribution, and origin of authigenic lithologies, in: C.K. Paull, P.W. Dillon (Eds.), Natural Gas Hydrates: Occurrence, Distribution, and Dynamics, Geophys. Monog. 124, 2001, pp. 99–113.

[5] E. Suess, G. Bohrmann, R. v. Huene, P. Linke, K. Wallmann, S. Lammers, H. Sahling, G. Winckler, R.A. Lutz, D. Orange, Fluid venting in the eastern Aleutian subduction zone, J. Geophys. Res. 103 (1998) 2597–2614.

[6] J. Greinert, Rezente submarine Mineralbildungen: Abbild geochemischer Prozesse an aktiven Fluidaustrittsstellen im Aleuten- und Cascadia-Akkretionskomplex, Dissertation, Christian-Albrechts-Universität Kiel, GEOMAR Report 87, 1999, 196/21 pp. (in German).

[7] T. Nähr, D.S. Stakes, W.S. Moore, Mass wasting, ephemeral fluid flow, and barite deposits on the California continental margin, Geology 28 (2000) 315–318.

[8] B. Fu, P. Aharon, G.R. Byerly, H.H. Roberts, Barite chimneys on the Gulf of Mexico slope: Initial report on their petrography and geochemistry, Geo-Mar. Lett. 14 (1994) 81–87.

[9] M.E. Torres, H.J. Brumsack, G. Bohrmann, K.C. Emeis, Barite fronts in continental sediments: A new look at barium remobilization in the zone of sulfate reduction and formation of heavy barites in authigenic fronts, Chem. Geol. 127 (1996) 125–139.

[10] M.E. Torres, G. Bohrmann, E. Suess, Authigenic barites and fluxes of barium associated with fluid seeps in the Peru subduction zone, Earth Planet. Sci. Lett. 144 (1996) 469–481.

[11] N.V. Astakhova, Hydrothermal Barite in the Okhotsk Sea, Resour. Geol. Spec. Issue 17 (1993) 169–172.

[12] N.V. Astakhova, Barite mineralization in sediments of the West Pacific marginal seas, Geol. Pac. Ocean 13 (1997) 945–955.

[13] A.N. Derkachev, G. Bohrmann, J. Greinert, A.V. Mozherovsky, Authigenic calcite and barite mineralization in sediments from Derugin basin, Sea of Okhotsk (in Russian), Lithol. Miner. Resour. 6 (2000) 568–585.

[14] G.S. Gnibidenko, Tectonics of the Seafloor from the Far East Marginal Seas, Nauka, Moscow, 1979, 163 pp. (in Russian).

[15] A.V. Zhuravlev, Comparison features for the Derugin and Tinro Basins in the Sea of Okhotsk (in Russian), Pac. Geol. 4 (1984) 21–27.

[16] P.M. Sychev, Main stages of the geological development in the Sea of Okhotsk and adjacent regions, in: K.F. Sergeev (Ed.), Geodynamics of Tectonosphere of the Pacific–Eurasia Conjunction Zone, Part VIII, Yuzhno-Sakhalinsk, 1997, pp. 169–190 (in Russian).

[17] O.J. Koblenz-Mischke, Primary production of the Pacific Ocean, in: M.E. Vinogradov (Ed.), Biology of the Pacific Ocean, Part 1, Nauka, Moscow, 1967, pp. 62–65 (in Russian).

[18] V.G. Bogorov, Plankton of the World Ocean, Nauka, Moscow, 1974, 320 pp. (in Russian).

[19] N. Biebow, E. Hütten, Cruise Report: KOMEX I and II (RV Gagarinsky; RV Lavrentyev), GEOMAR Report 82, 1999, 270 pp.

[20] N. Biebow, T. Lüdmann, B. Karp, R. Kulinich, Cruise Report: KOMEX III and IV (RV Gagarinsky; RV Gelovany), GEOMAR Report 88, 2000, 296 pp.

[21] F. Yanagisawa, H. Sakai, Thermal decomposition of barium sulfate-vanadium pentaoxide-silica glass mixture for preparation of sulfur dioxide in sulfur isotope ratio measurements, Anal. Chem. 55 (1983) 985–987.

[22] A.I. Obzhirov, Gas and Geochemical Fields of the Benthic Layer of Seas and Oceans, Nauka, Moscow, 1993, 131 pp. (in Russian).

[23] C.R. Fisher, Chemoautotrophic and methanotrophic symbioses in marine invertebrates, Rev. Aquat. Sci. 2 (1990) 399–436.

[24] P. Lonsdale, A deep-sea hydrothermal site on a strike-slip fault, Nature 281 (1979) 531–534.

[25] W.S. Moore, D. Stakes, Ages of barite-sulfide chimneys from the Mariana Trough, Earth Planet. Sci. Lett. 100 (1990) 265–274.

[26] C. Buczynski, S. Chafets, Habit of bacterially induced precipitates of calcium carbonate and the influence of medium viscosity on mineralogy, J. Sedim. Petrol. 61 (1991) 226–233.

[27] M.T. Gonzalez-Munoz, K. Ben Chekroun, A. Ben Aboud, J.M. Arias, M. Rodriguez-Gallego, Bacterially

induced Mg-calcite formation: Role of Mg^{2+} in development of crystal morphology, J. Sedim. Res. 70 (2000) 559–565.
[28] S.A. Gorbarenko, A.N. Derkachev, A.C. Astakhov, J.R. Sauton, D. Nuernberg, V.V. Shapovalov-Chuprynin, Lithostratigraphy and tephrachronology of the Upper Quaternary deposits in the Sea of Okhotsk (in Russian), Pac. Geol. 19 (2000) 58–72.
[29] K.S. Habicht, D.E. Canfield, Sulphur isotope fractionation in modern microbial mats and the evolution of the sulphur cycle, Nature 382 (1996) 342.
[30] Y. Mizutani, T.A. Rafter, Isotopic behavior of sulfate oxygen in the bacterial reduction of sulfate, Geochem. J. 6 (1973) 183–191.
[31] M.B. Goldhaber, I.R. Kaplan, Mechanisms of sulfur incorporation and isotope fractionation during early diagenesis in sediments of the Gulf of California, Mar. Chem. 9 (1980) 95–143.
[32] P. Fritz, G.M. Basharmal, R.J. Drimme, J. Isben, R.M. Qureshi, Oxygen isotope exchange between sulfate and water during bacterial reduction of sulfate, Chem. Geol. 79 (1989) 99–105.
[33] K.S. Habicht, D.E. Canfield, Sulfur isotope fractionation during bacterial sulfate reduction in organic-rich sediments, Geochim. Cosmochim. Acta 61 (1997) 5351–5361.
[34] R.M. Lloyd, Oxygen isotope behavior in sulfate-water system, J. Geophys. Res. 73 (1968) 6099–6110.
[35] G.E. Claypool, W.T. Holser, I.R. Kaplan, H. Sakai, I. Zak, The age curve of sulfur and oxygen isotopes in marine sulfate and their mutual interpretation, Chem. Geol. 28 (1980) 199–260.
[36] L. Aquilina, A.N. Dia, J. Boulègue, J. Bourgois, A.M. Fouillac, Massive barite deposits in the convergent margin off Peru: Implications for fluid circulation within subduction zones, Geochim. Cosmochim. Acta 61 (1997) 1233–1245.
[37] B.B. Jørgensen, A thiosulfate shunt in the sulfur cycle of marine sediments, Science 249 (1990) 152–154.
[38] E. Suess, M.J. Whiticar, Methane-derived CO_2 in pore fluids expelled from the Oregon Subduction Zone, Palaeogeogr. Palaeoclim. Palaeoecol. 71 (1989) 119–136.
[39] G.P. Sandimirova, Geochemical factors of Sr distribution and variations of its isotopic composition in hydrothermal systems, in: The Structure of the Hydrothermal System, Nauka, Moscow, 1993, pp. 196–218 (in Russian).
[40] A. Paytan, M. Kastner, E.E. Martin, J.D. MacDougall, T. Herbert, Marine barite as a monitor of seawater strontium isotope composition, Nature 366 (1993) 445–449.
[41] H. Elderfield, J.M. Gieskes, Sr isotopes in interstitial waters of Deep Sea Drilling Project cores, Nature 300 (1982) 493–497.
[42] S.E. Humphris, R.A. Zierenberg, L.S. Mullinneaux, R.E. Thomson, Seafloor hydrothermal systems: Physical, chemical, biological and geological interactions, AGU Geophys. Monogr. 91 (1995) 466 pp.